LA-UR -80-1796

CONF-800655--8

TITLE: RAPID FUEL DRAWER SCANNER FOR FAST CRITICAL ASSEMBLY SAFEGUARDS

AUTHOR(S): J. C. PRATT, S. W. FRANCE, H. H. HSU, J. T. CALDWELL, R. D. HASTINGS, E. R. SHUNK

MASTER

SUBMITTED TO: INMM 21st Annual Meeting
June 30-July 2, 1980
Palm Beach, Florida

University of California

LOS ALAMOS SCIENTIFIC LABORATORY
Post Office Box 1663 Los Alamos, New Mexico 87545
An Affirmative Action/Equal Opportunity Employer

Form No. 836 R3
St. No. 2629
12/78

UNITED STATES
DEPARTMENT OF ENERGY
CONTRACT W-7405-ENG 36

RAPID FUEL DRAWER SCANNER FOR FAST CRITICAL ASSEMBLY SAFEGUARDS

J. C. Pratt, J. T. Caldwell, S. W. France, R. D. Hastings,
H. H. Hsu, and E. R. Shunk

Los Alamos Scientific Laboratory
Los Alamos, New Mexico, 87545

ABSTRACT

An integrated scanning system incorporating highly efficient collimated neutron and high purity germanium gamma detectors with an on-line microprocessor has been developed to perform rapid inventorying of uranium and plutonium fuel drawers from fast critical assemblies. On-line least-squares fit procedures provide quantitative comparisons at a rate exceeding two drawers per minute. For plutonium-containing fuel, the neutron scan data can be related to the included ^{240}Pu isotopic mass; individual ^{239}Pu, ^{241}Pu, and ^{241}Am isotopic contents are obtained from simultaneous scans of the appropriate isolated gamma lines.

With world-wide research employing fast critical assemblies, the question arose in recent years as to how a facility's fuel inventory could be verified in a timely fashion. Generally, fuel at a critical assembly will be well characterized with precisely specified physical form and material content. These facilities will generally have elaborate physical security and inventory measures which can instantly specify the location of individual fuel coupons. However, with potentially substantial quantities "in use" in the assembly for relatively long periods, there is the question of verification that fuel is actually present. To the facility operator, that is really no problem because his performance prediction and instrumentation would probably show discrepancies if there were any material missing. To an outside observer/inspector (who can make no independent prediction or whose independent instrumentation of the assembly could not practically approach that of the facility operator), some other verification must be available. Hopefully that verification could be planned to minimize inconvenience to the facility operator and maximize the inspector's effectiveness. Los Alamos Scientific Laboratory (LASL) Group Q-2 has begun development of a system for scanning fast critical assembly (FCA) fuel drawers. In concept, a conveyor belt carries the drawer past a collimated high-efficiency neutron detector and a collimated high-resolution gamma detector. A schematic of the scanner is shown in Fig. 1. The neutron detector is housed in a polyethylene collimator assembly and it consists of twelve ^{3}He proportional counters. The

individual ^{3}He tubes have 51-mm diameter, 419-mm length of active volume, and a fill pressure of 3 atm. The measured neutron detection efficiency is approximately 5% and the measured spatial full width at half maximum (FWHM) is approximately 50 mm. The gamma detector is a high-purity germanium detector, with a detection efficiency of 20% of the efficiency of a 75-mm x 75-mm NaI(T) detector. The gamma detector collimator gives a FWHM of about 10 mm. The system is designed to scan typical fuel drawers at a rate of one or two per minute, with a sensitivity adequate to detect the presence or absence of a typical 1-in.-long plutonium fuel plate in a drawer containing as much as 36 in. (total) of plutonium fuel in one or more rows and a variety of coolant, structural, and fertile mockup materials also present in the drawer.

The technique assumes that the plutonium fuel plates in the facility inventory are well characterized, but it does not require that all fuel plates have the same ^{240}Pu, ^{241}Am, etc., isotopic content. An example of possible fuel inventory variation is shown in Table I. Table II shows the measured or calculated neutron and isotope-specific gamma intensities for the plutonium fuel plates listed in Table I. The neutron and gamma line intensities are tabulated as relative values per inch of fuel plate, with the Pu/U/Mo fuel of 11.56% ^{240}Pu content arbitrarily designated as the unity response.

TABLE I

TYPICAL ISOTOPIC VALUES FOR FIVE CLASSES OF PLUTONIUM FUELS IN A CRITICAL FACILITY

Fuel Type	^{239}Pu (%)	^{240}Pu (%)	^{241}Pu (%)	^{241}Am (%)	Plutonium Per Inch (g)
Pu/Al	95.25	4.50	0.20	0.24	34.1
Pu/U/Mo	90.80	8.66	0.51	0.46	20.0
Pu/U/Mo	87.00	11.56	1.20	0.59	31.1
Pu/Al	74.20	22.23	2.86	1.80	35.3
Pu/U/Mo	68.70	26.40	3.39	2.19	37.7

TABLE II

MEASURED (OR CALCULATED) NEUTRON AND GAMMA RESPONSES FOR FIVE CLASSES OF PLUTONIUM FUELS

Fuel Type	^{240}Pu (%)	Rel. Total Neut. per Inch	Rel. Total ^{239}Pu (414 keV /in.)	Rel. Total ^{241}Am (662 kev /in.)
Pu/Al	4.50	0.73 ± 0.07	(1.26 ± 0.13)	(0.42 ± 0.04)
Pu/U/Mo	8.66	0.47 ± 0.05	(0.67 ± 0.07)	(0.49 ± 0.05)
Pu/U/Mo	11.56	1.00 ± 0.10	1.00 ± 0.10	1.00 ± 0.10
Pu/Al	22.33	3.17 ± 0.32	0.96 ± 0.10	3.44 ± 0.30
Pu/U/Mo	26.40	(2.75 ± 0.28)	(0.95 ± 0.10)	(4.47 ± 0.45)

Each class of plutonium fuel has a characteristic signature when the three independent quantities (total neutron, ^{239}Pu, ^{241}Am) are considered. Furthermore, based on our experimental measurements with 25 separate fuel plates taken from among the first four classes listed in Table II, the uniformity of signature from plate to plate within a class appears to be quite good. This uniformity is probably due to the excellent quality control required in the manufacture of such plates. The Pu/U/Mo plates have a neutron output consistent with 100% spontaneous fission, and the Pu/Al plates have an additional Al (α,n) component (~70% for the 4.50% ^{240}Pu plates and 50% for the 22.33% ^{240}Pu plates).

We have used this scanner for preliminary data acquisition at the Zero Power Plutonium Reactor (ZPPR) at the Argonne West facility at Idaho National Engineering Laboratory. For this preliminary data acquisition, we fixed the scanner belt speed at 25 mm/s and we simultaneously acquired four scans of each drawer with a data point in each scan each 0.5 seconds. The data acquired for each of the four scans are as follows:

a) One for the gross neutron signal, which is proportional to ^{240}Pu content.

b) A gross gamma-ray signal (200- to 800-keV window).

c) A ^{241}Am-^{241}Pu gamma-line window (208-keV line is used).

d) A ^{239}Pu gamma-line window (the 375- and 414-keV lines are used).

A plot of this energy region in the gamma-ray spectrum is shown in Fig. 2.

We arranged our visit for a time when the ZPPR fuel loading was being modified and this allowed an opportunity to scan a number of fuel drawers. Unfortunately, this opportunity came before the delivery of the Data General NOVA 4 planned for this use; we made these scans with a microNOVA that ran the programs planned for the NOVA. For this trip our data acquisition program was designed to acquire, store, and compare the scans. We wrote a program with a real-time multi-task architecture, which acquired scans and simultaneously analyzed the previous scans. The analysis calculations allowed comparison with any previous scan recorded on the disk. For each of the four data channel scans we calculated a background-subtracted integral and FWHM. Then the individual channel's scan and that channel's scan of its comparison file were compared by calculation of the RMS difference of the fractions in each of the 0.5-s data points. Photographs of the scanner and its data acquisition equipment in use at the ZPPR are shown in Figs. 3a and 3b. The on-line printout is shown in Fig. 3b for a single drawer.

A part of the data recorded on diskette for each scan was the clock time elapsed between the interruption of "electric eye" light sensors located at fixed points on the scanner. All scan data were recorded at the fixed rate of 0.500 s per channel. Thus, by obtaining the scan velocity from the light sensor data, we were able to determine the observed scan widths (FWHM for net data) and to compare them to the actual length of fuel plates in the drawer. For example, the scan speed for the data shown in Fig. 4 was 0.945 in. per second. The observed FWHM's for the four scans were 42.2, 42.3, 42.5, and

42.7 channels, respectively, for the gross neutron, gross gamma, ^{241}Am gamma line, and ^{239}Pu gamma lines. The corresponding total fuel plate lengths calculated for these data are 19.93-, 19.98-, 20.07-, and 20.17-in., respectively, all of which correspond closely to the physical fuel plate extent of 20 inches. We have calculated the FWHM for a number of the scans we took at ZPPR and have observed the same close correspondence between FWHM and physical fuel plate extent for all scans.

The operator had the option of making hard-copy plots of the scan comparisons. On-line plots are shown in Fig. 4. The first is the neutron scan. The spatial resolution of that scan is about 50 mm, so the spatial details of this tray are not visible. This tray is a double-row tray with each row containing one 7-in., one 5-in. and two 4-in. plates. That structure is visible in the second scan, the gross gamma-counts channel. The program was told to compare the tray with itself so the pictures will show the tray's features most clearly. The dips in the top of the scan correspond to the plate boundaries, and the plate order apparent in the scan is 7-5-4-4. The scans with narrower windows, the third and fourth ones shown in Fig. 4 (the scans for the $^{241}Am/^{241}Pu$ lines at 208 keV and the ^{239}Pu complex around 375- and 414-keV), show the same structure.

Figure 5 shows the result of scanning one tray twice and comparing the two measurements. This tray has two rows of fuel plates, first row 7-, 5-, 4-, and 4-in. ZPPR plates; second row 3-, 3-, 3-, 3-, 3-, 2-, 1-, and 2-in. Pu-Al plates. Figure 5a is the gross gamma-counts scan, with the on-line comparison RMS difference of 0.00607. The second plot in Fig. 5b is the result of scanning the tray again with the 1-in. plate removed. The RMS difference comparing that scan with the original scan was 0.01362, which was considerably greater than the comparison for the scan with one 1-in. plate in place. The position of the missing 1-in. plate is clearly visible in the scan. The other two gamma scans ($^{241}Pu/^{241}Am$ line, ^{239}Pu lines) display the same feature, a highly visible dip at the position of the missing plate.

Gross neutron scan comparisons are shown in Figs. 6a and 6b. Figure 6a shows the neutron scan pair corresponding to the gross gamma scans of Fig. 5a. The RMS deviation for the shape fit comparisons of two passes of the same drawer (Fig. 6a) is 0.00977. Figure 6b shows a comparison between one of the scans of Fig. 6a and a scan in which a 2-in. Pu-Al plate has been removed from one row. The removal is evident visually (centered at approximately Channel 54) and results in an RMS deviation value (0.01370) considerably larger than for comparisons of full drawers.

In addition, the scan integral neutron count obtained for the "missing plate" drawer is lower (24604) than for the full drawer (25884). Although the corresponding neutron scan with only one 1-in. plate missing does not show a qualitatively evident dip at the position of the missing material, the RMS deviation (0.01288) and scan integral count (24915) quantitatively distinguish it from the full drawer scan.

In our visit to ZPPR we obtained almost 200 tray scans. On the busiest day, we scanned about 100 trays, approximately half the trays handled by the facility. On that day the facility used automated tray-handling equipment.

The possibilities of increasing belt speed to 50 mm/s and organizing the scanning to allow more than one tray on the scanner at a time might increase the drawer verification rate to 75-100 per hour.

The ZPPR visit allowed us to scan 22 different drawer loadings. These included both single-row and double-row drawers and three different plate alloys. The sums of the materials in the drawers as a whole fell into five groups with compositions shown in Table III. Considering only the background-subtracted integrals and the FWHM to produce the counts-per-inch for each of the four channels, the values for each of those five drawer-loading families are shown in Figs. 7a-d.

TABLE III

TRAY ASSAY FAMILIES

Tray Family	Total Pu (g)	^{239}Pu (g)	^{240}Pu (g)	^{241}Pu (g)	^{241}Am (g)
A_1	1314	1198	103.6	8.8	5.3
A_2	1250	1088	144.6	7.4	15.0
A_3	1024	906	106.8	5.6	9.5
A_4	398.6	361.9	34.5	1.9	2.0
A_5	628.4	547	72.7	3.7	7.6

The plots in Fig. 7 seem to show that no single measurement might distinguish all five cases unambiguously, but the combination of all four measurements should allow clear discrimination. In fact, with later off-line analysis we investigated this method of tray identification. Defining a four-dimensional metric space with distances measured in units of the statistical errors of the scan, we selected the tray-family identification with the smallest distance between that tray and the tray-family characterization point. Using this method an off-line analysis program correctly identified the tray-type for 166 out of 166 trays.

The relationship between the integrals and the quantities of materials in the tray is investigated in Fig. 8a-d. The first plot (Fig. 8a) compares the neutron counts with the ^{240}Pu content. Note the effect of the Pu-Al alloy plates in the first tray-analysis family. The second plot (Fig. 8b) compares the gross gamma count and the total plutonium mass. The third plot (Fig. 8c) compares the count in the $^{241}Am/^{241}Pu$ window with the ^{241}Pu mass. The fourth plot (Fig. 8d) similarly compares ^{239}Pu mass and the counts in the ^{239}Pu window.

One reason for the choice of the high-resolution gamma-ray detector was the possibility that the tray scan might occur at any time in the operational cycle of the FCA, and so the fuel might contain fresh fission fragments. Ideally the verification results would not be effected by these. Of course the fission fragment inventory is much smaller in research FCA facilities compared to power reactors, and Fig. 9 gives some idea of this effect in the gamma ray spectrum. Notice that the bulk of the fission fragment photopeaks is above the region used for these measurements. Still, a large fission-

fragment inventory could provide a gamma-ray buildup at the lower energies. Of course the neutron scan is not effected. In order to see if the influence of this potential variation in tray signature could be minimized, we used the limited range of fission fragment gamma activity available in our scan data. Selecting the trays in each assay family with the largest variation in gross counts, we fitted straight lines to the narrow-window counts as a function of the gross count. In that narrow window the photopeak sits on a background presumed proportional to the gross counts. This gave us a new characterization of each of the tray families that corresponded to the zero-background (pure photopeak) signal. These were used to define a three-dimensional metric space used for tray-family identification like the four-dimensional space. Again, this method correctly selected the tray family for 166 out of 166 tray scans.

In summary, this drawer scanner can examine FCA fuel at a rate of 25.4 mm/s, simultaneously collecting neutron and gamma-ray information for a total of four scans. The length of the neutron and gamma-ray emitting material is accurately determined. The count integrals of the four scans allow identification of the total tray loading of ^{239}Pu, ^{240}Pu, and ^{241}Pu. We are continuing our analysis of the data to investigate the sensitivity of the integrals to the mass present. Perhaps we can correlate the information in the scan integrals to achieve detection of the absence of the smallest fuel plate in the inventory based on those integrals alone. Finally, we have the spatial scans themselves that clearly show the absence of single plates and the location that the material came from (Figs. 5-6). We are investigating analysis methods to extract this information from the scans and correlate those results from all the scans for maximum sensitivity and convenience.

We plan continued development of this scanner with the goal of a machine that performs a conceptually simple measurement with straightforward interpretation that yields immediate results.

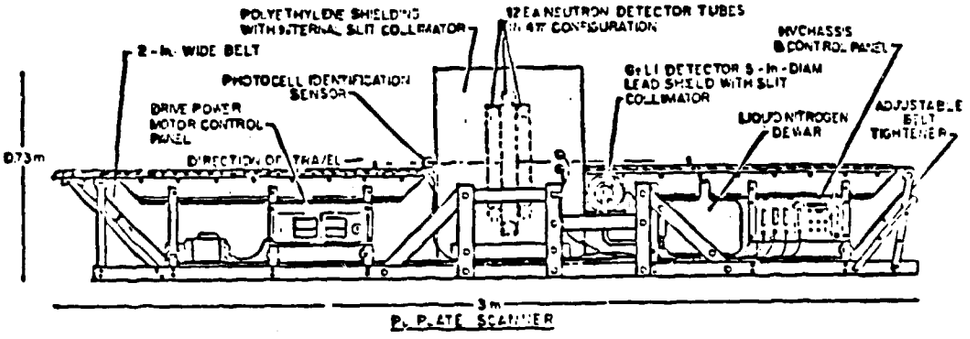

Fig. 1. Schematic of FCA fuel drawer scanner.

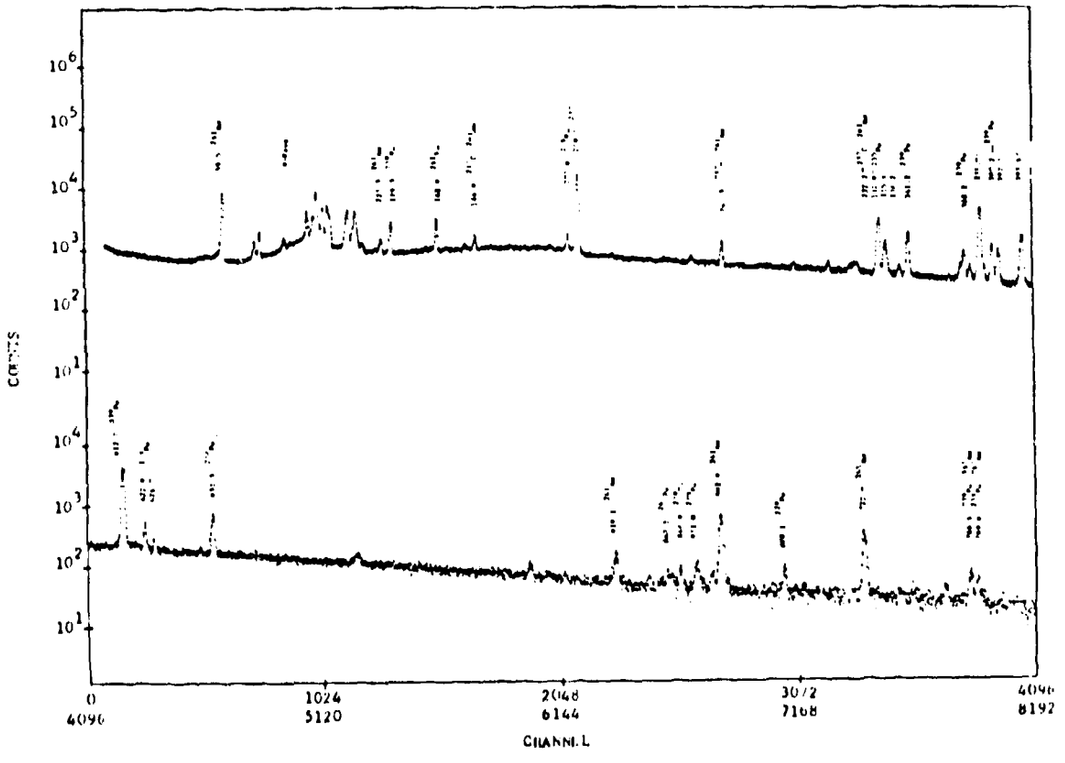

Fig. 2. Gamma-ray spectrum from the high-purity germanium gamma-ray detector showing the region in which the gamma-ray scan windows were chosen.

Fig. 3a. Scanner and data acquisition equipment in operation at ZPPR.

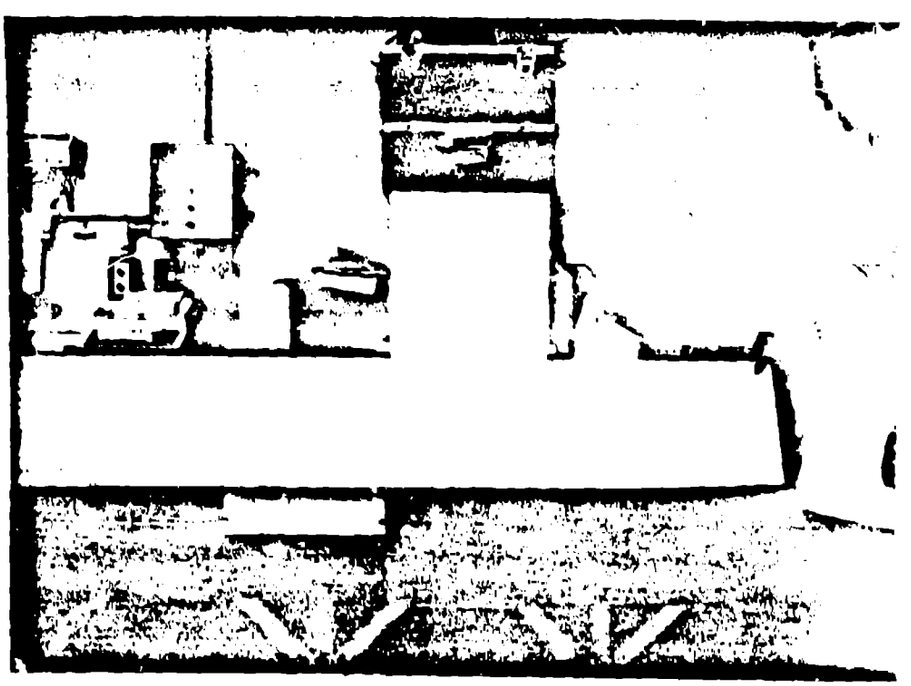

Fig. 3b. Scanner with on-line plot from a single tray's scan.

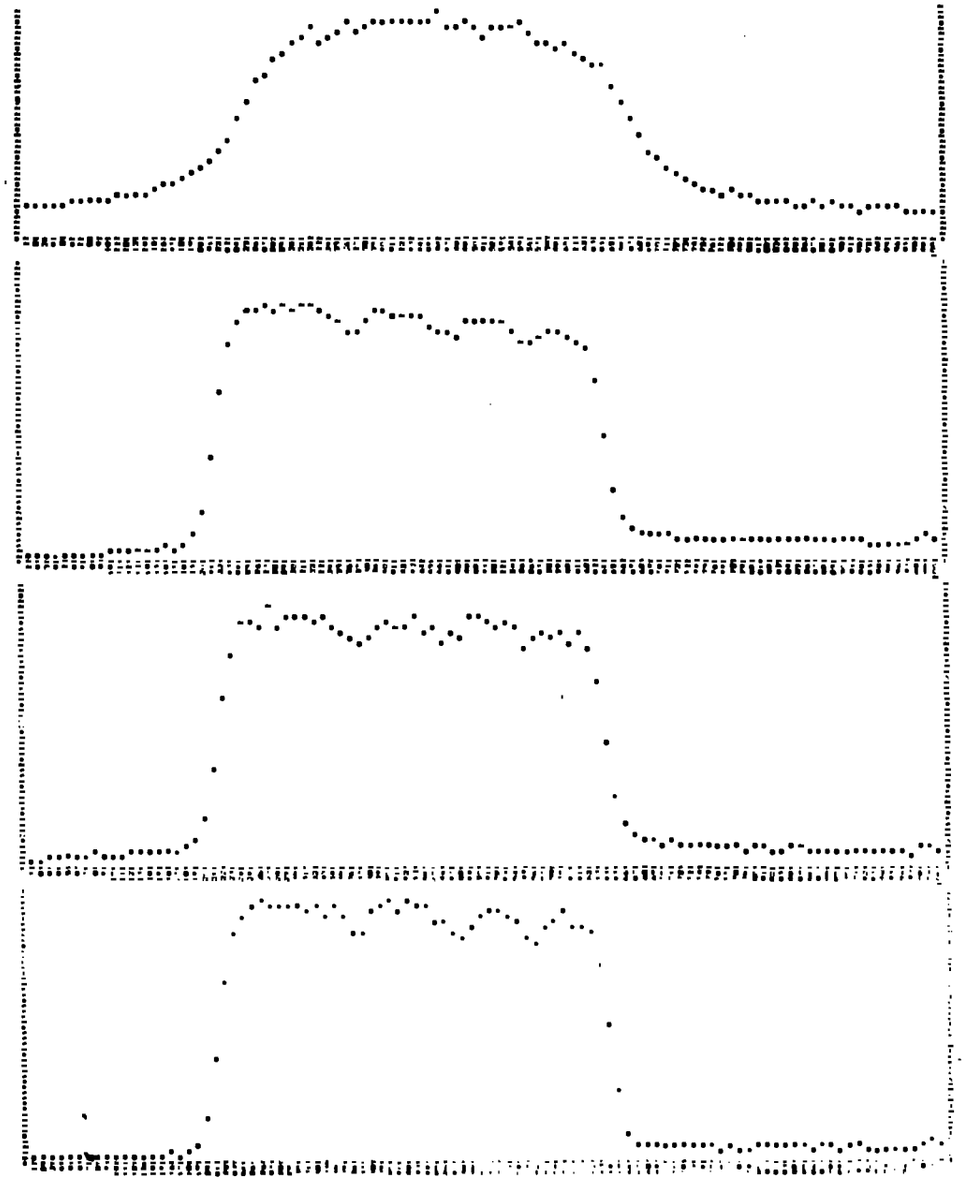

Fig. 4. On-line plots reading from top to bottom: neutron scan, gross gamma counts, $^{241}Am/^{241}Pu$ window at 208 keV, ^{239}Pu window.

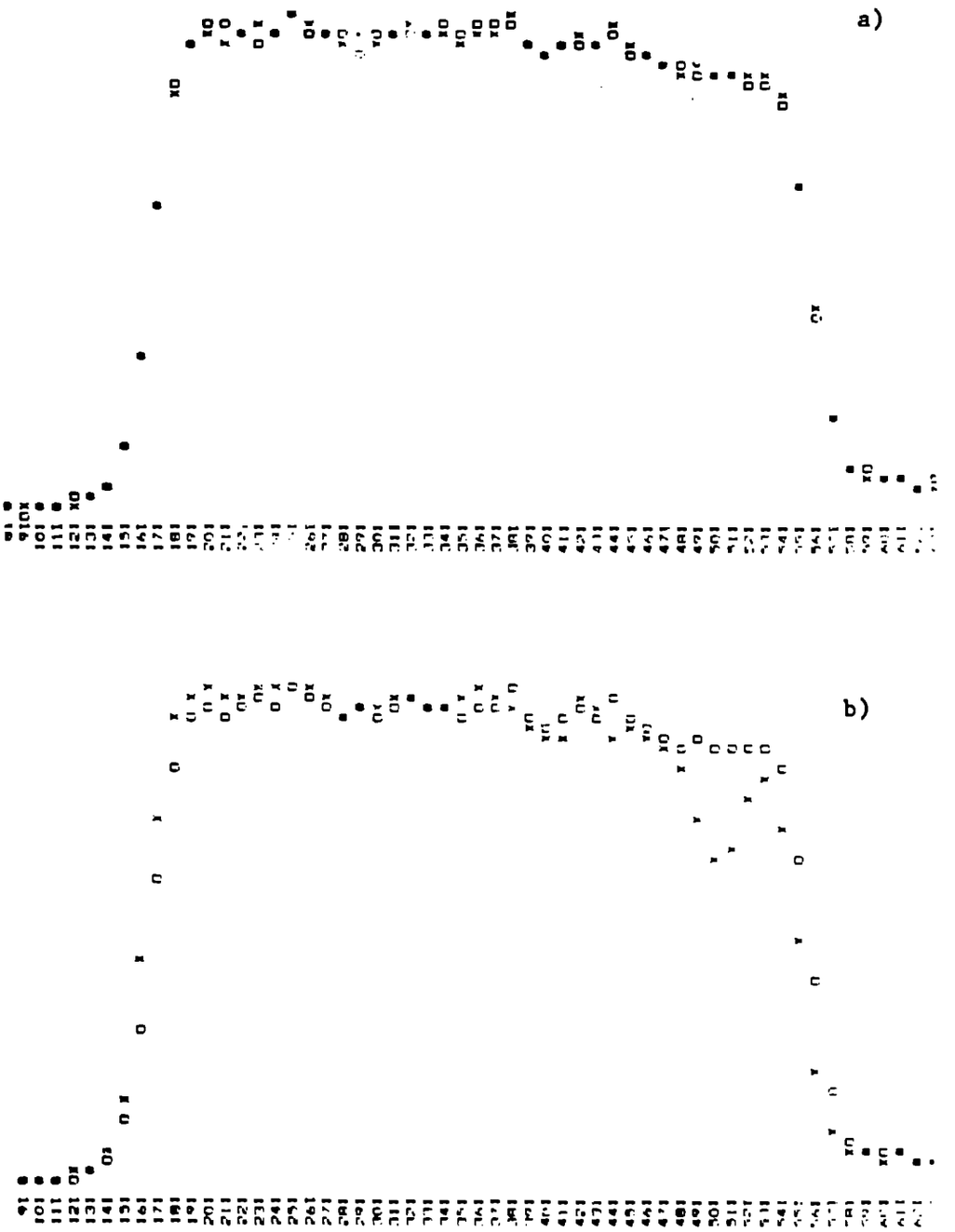

Fig. 5. On-line plots, gross gamma scan, from:

a) Two independent scans of the same tray.

b) Two scans of the same tray, one of which has a 1-in. Pu-Al plate removed.

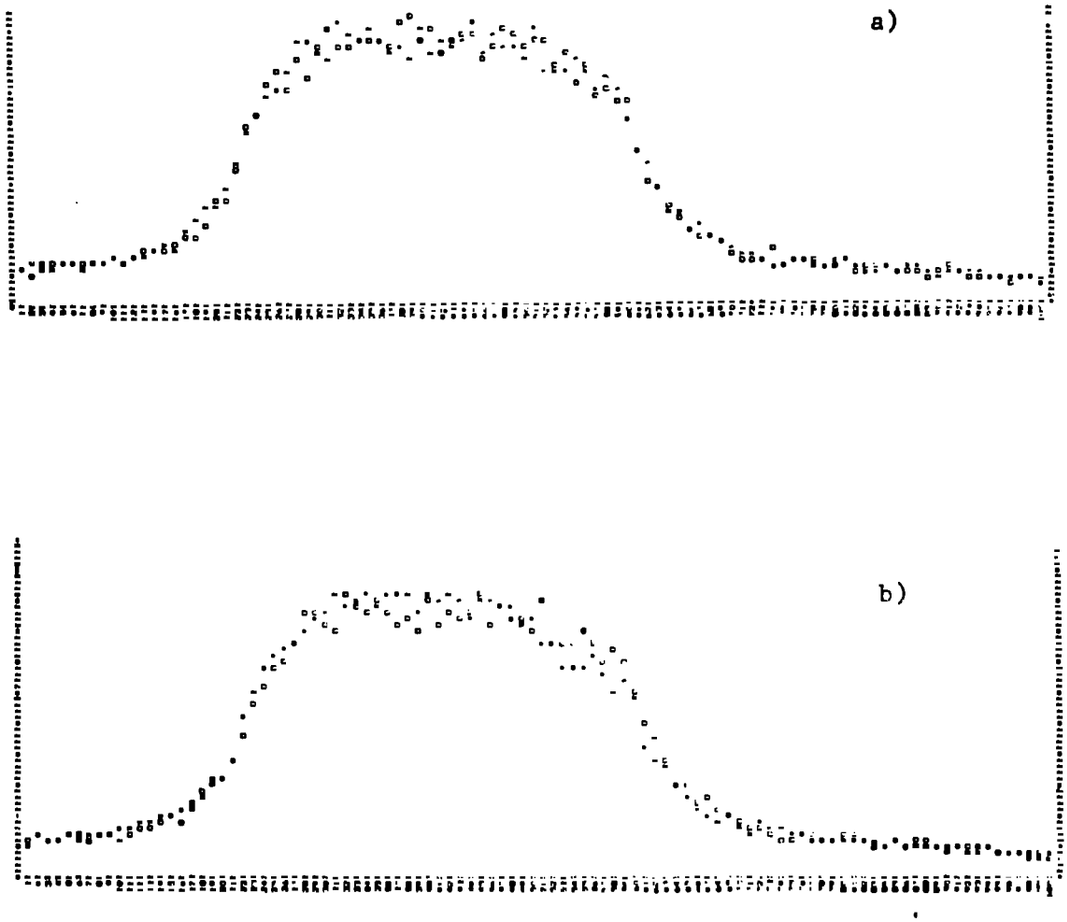

Fig. 6. On-line plots, neutron scan, from:

a) Two independent scans of the same tray.

b) Two scans of the same tray, one of which has a 2-in. Pu-Al fuel plate removed.

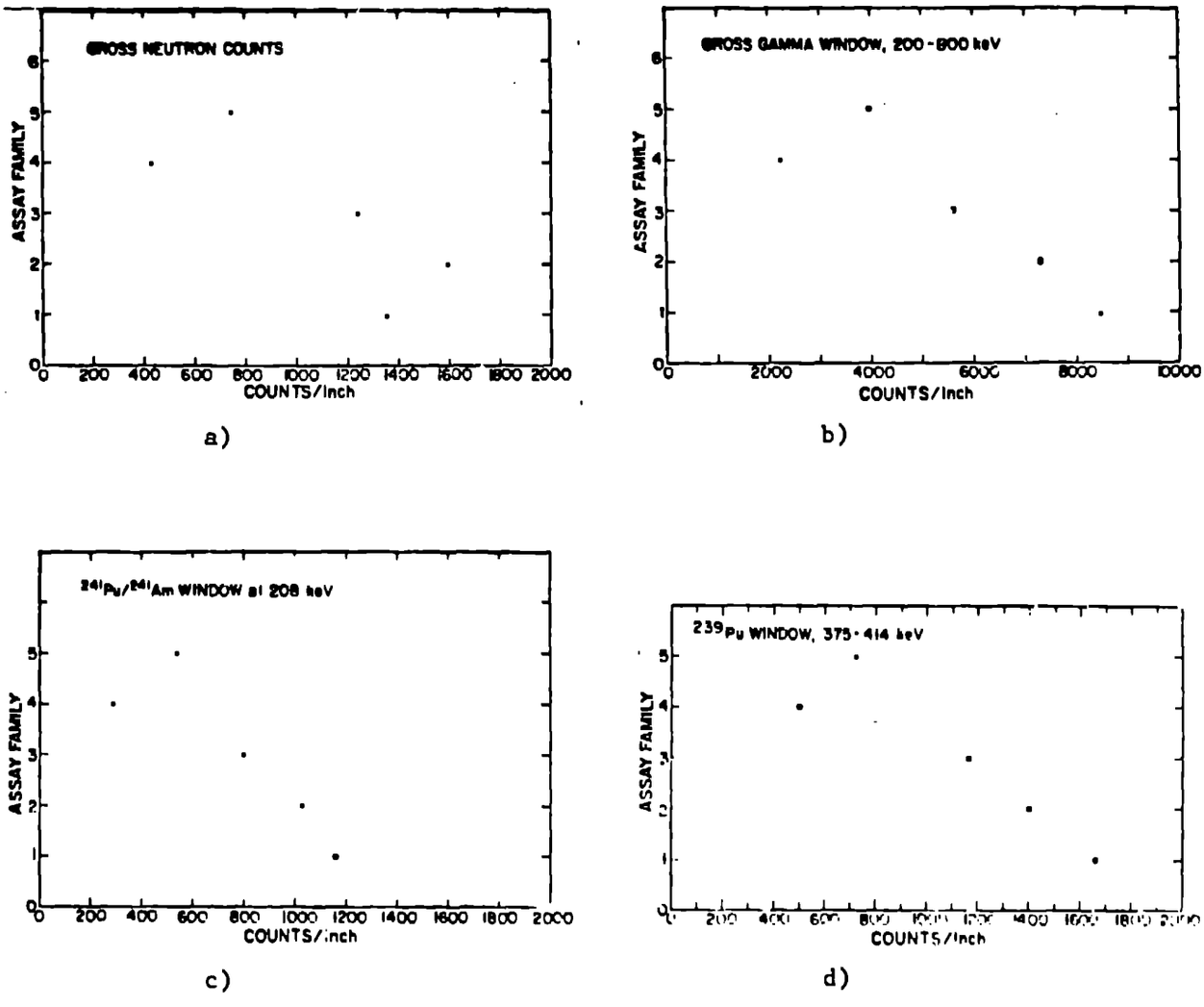

Fig. 7. Scan integrals, average of the trays in each analysis-family of Table III.

a) Neutron scan.

b) Gross gamma scan.

c) 208-keV gamma window scan.

d) 375- to 414-keV gamma window scan.

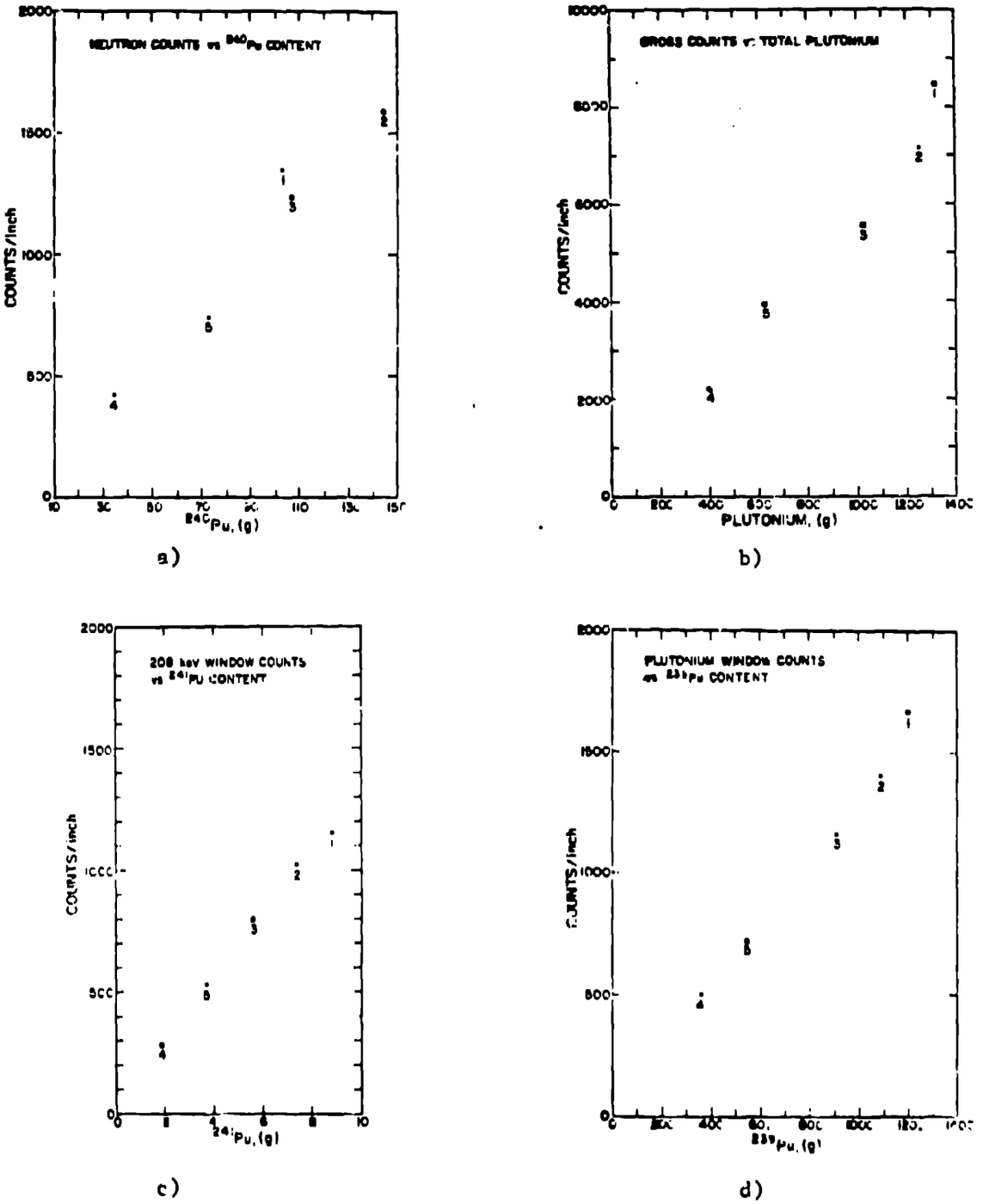

Fig. 8. Scan integrals compared with plutonium mass for each of the four scans:

a) Neutron scan.
b) Gross gamma scan.
c) 208-keV gamma window scan.
d) 375- to 414-keV gamma window scan.

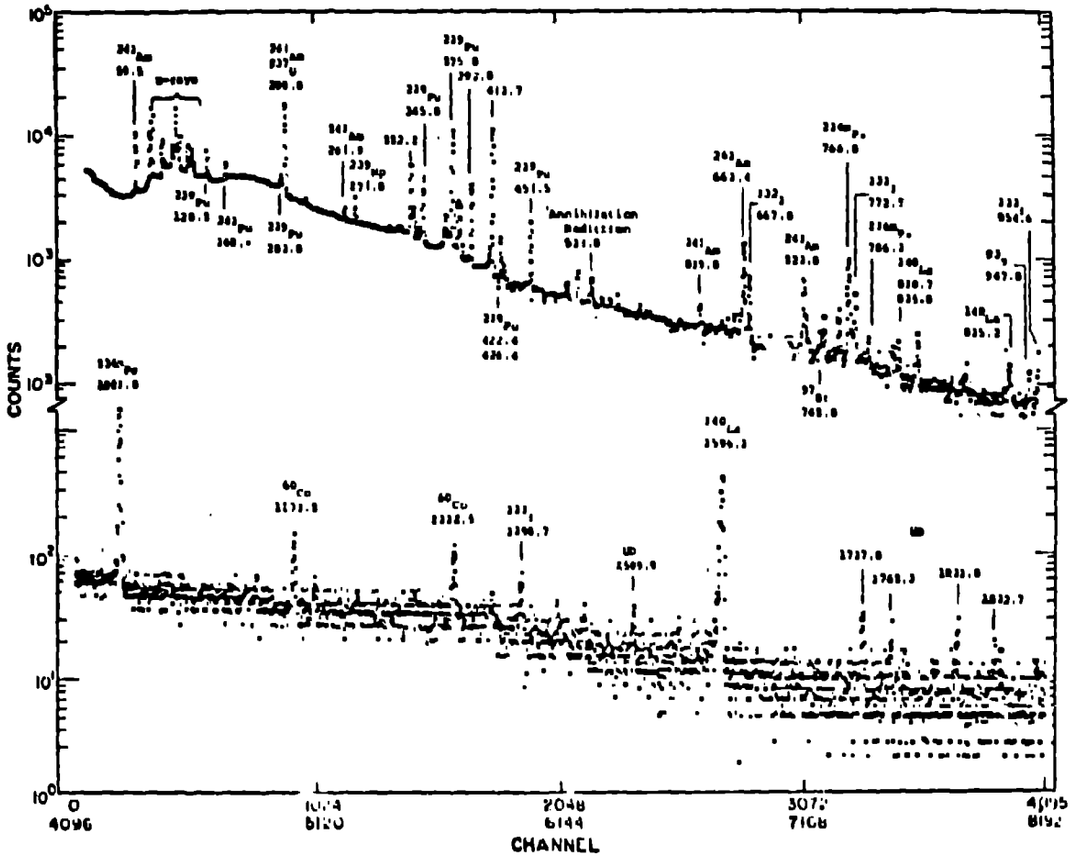

Fig. 9. Gamma ray spectrum, showing fission-fragment gamma rays and plutonium gamma rays.